

Driving rotamak currents with minimal power dissipation

Cite as: Phys. Plasmas **28**, 122504 (2021); doi: 10.1063/5.0070425

Submitted: 6 September 2021 · Accepted: 28 November 2021 ·

Published Online: 28 December 2021



J. J. Van De Wetering^{1,2,a)} and N. J. Fisch³

AFFILIATIONS

¹Department of Physics, Princeton University, Princeton, New Jersey 08544, USA

²Department of Physics, University of Oxford, Oxford OX1 3RH, United Kingdom

³Department of Astrophysical Sciences, Princeton University, Princeton, New Jersey 08544, USA

^{a)}Author to whom correspondence should be addressed: johannes.vandewetering@physics.ox.ac.uk

ABSTRACT

The *Rotamak* is a proposed thermonuclear fusion device which employs rotating magnetic fields (RMF) to generate an azimuthal current to produce a field-reversed configuration. The efficiency of the currents that produce the field reversal by RMFs was debated some 40 years ago. The debate revolved around whether the currents would incur dissipation by the conventional Spitzer perpendicular resistivity, or whether some other relation between current and dissipation would be more appropriate. By employing an electron–ion pitch-angle scattering model, we find that the dissipation is non-Spitzer in nature. However, curiously, there appears to exist a regime where the power dissipated to maintain the current becomes vanishingly small.

Published under an exclusive license by AIP Publishing. <https://doi.org/10.1063/5.0070425>

I. INTRODUCTION

The *Rotamak* is a proposed device for thermonuclear fusion which uses a rotating magnetic field perpendicular to an axial magnetic field driving an azimuthal current.^{1,2} The azimuthal current generates an axial field that tends to cancel the imposed axial magnetic field. This cancellation allows a field-reversed configuration (FRC) which has certain advantages for confining plasma. Experimental examples of this concept include the works of Hugrass *et al.*,³ Slough and Miller,⁴ Furukawa *et al.*,⁵ Guo *et al.*,⁶ and Cohen *et al.*⁷

The accepted picture for the generation of the azimuthal current is that highly magnetized electrons are tied to the magnetic field lines, so the electrons will rotate with the transverse rotating magnetic field (RMF). On the other hand, ions are not so magnetized, so they are left behind, thus leaving a net azimuthal current. This discrepancy between the electrons and ions is characterized by the two dimensionless parameters for each species,

$$\begin{aligned} p &= \frac{qB_0}{m\omega}, \\ w &= \frac{qB_{\perp}}{m\omega}, \end{aligned} \quad (1)$$

where q and m are the charge and mass of the particle, B_0 is the fixed axial field, B_{\perp} is the rotating field strength, and ω is the angular

frequency of the RMF. Due to the difference in mass between electrons and ions, it is possible to achieve large values for p_e , w_e while having small values for p_i , w_i to achieve this net azimuthal current.

The aim of this paper is to determine the power dissipated in the plasma as it is driven by the RMF to form the azimuthal current. In the considerations here, the RMF is assumed to penetrate the plasma fully, so that it is simply given as the vacuum rotating field. The matter of field penetration, though not considered here, will of course be of concern in a realistic setting.⁸ However, even with this simplification, the power dissipated is still not trivially calculated.

For our discussions, it will be useful to define the dimensionless efficiency parameter \mathcal{E} relative to the classical Spitzer resistivity,

$$\mathcal{E} = \frac{\eta_{sp} J_{\theta}^2}{P_D}, \quad (2)$$

where P_D is the power dissipated, J_{θ} is the azimuthal current, and $\eta_{sp} = \frac{m_e \nu_{ei}}{ne^2}$ indicates the classical Spitzer resistivity with electron–ion collision frequency ν_{ei} , which is defined later in Eq. (31). The controversy of efficiency of current drive by rotating waves revolves around how large/small this parameter is. The larger this parameter is, the more efficient the current drive.

Hugrass and Klima^{9–12} originally argued that as long as the RMF field strength $|w_e| \gg 1 \gg w_i$ is observed, then the electrons will

undergo “flux preserving motion”¹³ which effectively allows us to picture the electron fluid as frozen-in and rotating near-synchronously with the rotating field, while the ion fluid remains static. This, combined with a sufficiently low electron–ion collision rate relative to the gyrofrequency in relation to the rotating field (i.e., allowing a few orbits to occur before a collision event), Hugrass–Klima arrived at an efficiency cap of

$$\mathcal{E}_{HK} \lesssim 1, \tag{3}$$

which would be consistent with the picture of an electron fluid being dragged along with the RMF incurring Ohmic resistivity. Equality would only hold as the “slip” between the RMF and electron fluid rotation went to zero.

Fisch and Watanabe¹⁴ instead suggested that the picture of tying electrons to field lines in calculating an Ohmic-like power dissipation is an oversimplification. Taking into account that the electrons in a rotating field have coherent oscillatory energy, much greater than the average drift energy, could lead to larger randomized energy and power dissipation. That the electrons can have a large oscillatory energy is based simply on solving the equations of motion between collisions,^{15–17} which have analytic solutions. They found that good azimuthal current generation only occurs in the $w_e^2 \gg |p_e| \gg 1$ electron regime (with both ion quantities being small), and that its corresponding efficiency of

$$\mathcal{E}_{FW} = \frac{1}{|p_e|} \ll 1, \tag{4}$$

is far smaller than the classical Spitzer picture, suggesting that the rotamak concept may be impractical for current drive.

Hugrass disagreed with this method. His main criticism of Fisch–Watanabe was that their single particle orbit theory failed to take into account the relation between momentum and energy transfer during collisions as outlined by Klima.^{11,12} This would mean that one cannot simply conclude that the oscillating part of the electron orbits would all be lost due to collisions. On top of this, Hugrass⁹ also criticized the fact that Fisch–Watanabe did not consider all possible initial conditions in their analysis, instead opting to pick a specific orbit to represent the whole system.

In this paper, we follow the single-particle approach of Fisch–Watanabe but apply a more complete single-particle analysis, in which all electrons orbits are considered and undergo multiple stochastic isotropic pitch-angle scatterings with a fixed background of ions. Hence, instead of associating an oscillatory energy with an *average* single electron (as was done in Fisch–Watanabe), we actually consider the properties of many electrons over many collisions. We find that, in contrast to Fisch–Watanabe, that neither the use of a single representative *average* orbit nor the assumption of the oscillating energy being dissipated captures the actual power dissipation.

In considering multiple collisions and working in the $w_e^2 \gg |p_e| \gg |w_e| \gg 1$ regime to guarantee good current generation, it will turn out that a collection of electrons tends to a preferred speed-radius ratio, the dynamics of which determining short-term expansion-cooling/contraction-heating within a few collision times. After the system of electrons has settled into this preferred state, there will only remain very slow heating and expansion, resulting in a high current drive efficiency which greatly outperforms the Spitzer resistivity with an efficiency of

$$\mathcal{E} \approx |p_e| \gg 1. \tag{5}$$

In the first section, we begin by re-deriving and solving the equations of motion for a single particle in an RMF. Second, we introduce an electron–ion scattering model which treats electron pitch-angle scattering as instantaneous events which conserve energy and isotropize velocity. Considering all possible initial conditions, in the third section we calculate analytically how the average radius and speed of a large population of randomized electrons evolves under these collisions and compare this result with direct simulation. We then recover the overall long-term heating rate and azimuthal current, from which we can derive a novel resistivity law. We will find, in fact, a regime in which the power dissipation is far less than what either Fisch–Watanabe or Hugrass–Klima would predict.

II. SINGLE PARTICLE ORBITS IN A ROTATING MAGNETIC FIELD

A. Equations of motion

We will first re-derive the equations of motion found in the Fisch and Watanabe paper¹⁴ of a particle in an RMF with an axial magnetic field. A rotating magnetic field, \mathbf{B} , that is constant in the z -direction can be described as

$$\mathbf{B} = B_{\perp}(\cos(\omega t)\hat{x} + \sin(\omega t)\hat{y}) + B_0\hat{z}, \tag{6}$$

where B_{\perp} is the magnitude of the rotating magnetic field, B_0 is the constant axial magnetic field in the z -direction, and ω is the angular frequency of rotation.

We can find the RMF’s consistent E -field by using the Maxwell equations in a vacuum in SI units, two of which read

$$\begin{aligned} \nabla \cdot \mathbf{E} &= 0, \\ \nabla \times \mathbf{E} &= -\partial_t \mathbf{B}. \end{aligned} \tag{7}$$

Assuming no static E -field in the background this implies

$$\mathbf{E} = \omega B_{\perp}(x \cos \omega t + y \sin \omega t)\hat{z}. \tag{8}$$

However, there are two more Maxwell equations. The first is about the zero divergence of the magnetic field $\nabla \cdot \mathbf{B} = 0$, which is respected. The other (vacuum) Maxwell equation,

$$\nabla \times \mathbf{B} = \frac{1}{c^2} \partial_t \mathbf{E}, \tag{9}$$

is not respected. In order to satisfy the Ampère–Maxwell law corrections need to be made to the electromagnetic fields on order of $(\omega r/c)^2$ in relative size, where r is the radial distance to the z -axis. We will work in the non-relativistic limit and ignore these corrections.

The Lorentz force equation on a particle of mass m and charge q gives

$$m\ddot{\mathbf{r}} = q\mathbf{E} + q\dot{\mathbf{r}} \times \mathbf{B}, \tag{10}$$

where we use the dot notation for the time t derivative. This gives us

$$\begin{pmatrix} \ddot{x} \\ \ddot{y} \\ \ddot{z} \end{pmatrix} = \frac{q}{m} \begin{pmatrix} \dot{y}B_0 - \dot{z}B_{\perp} \sin \omega t \\ -\dot{x}B_0 + \dot{z}B_{\perp} \cos \omega t \\ B_{\perp} \frac{d}{dt}(x \sin \omega t - y \cos \omega t) \end{pmatrix}. \tag{11}$$

We introduce the dimensionless parameters, τ , p , and w , which are defined as

$$\begin{aligned} \tau &= \omega t, \\ p &= \frac{qB_0}{m\omega}, \\ w &= \frac{qB_{\perp}}{m\omega}, \end{aligned} \tag{12}$$

where p and w correspond to the axial field strength and RMF amplitude respectively as outlined in Eq. (1), and τ to the angle swept in time. For example, for the PFRC-2,^{29,30} for electrons we get $p_e = -8.9 \times 10^2$ and $w_e = -4.4 \times 10^1$. For protons, the parameters are $p_i = 4.8 \times 10^{-1}$ and $w_i = 2.4 \times 10^{-2}$.

Using τ for the dot derivative notation now (and not time t), we can rewrite

$$\begin{pmatrix} \ddot{x} \\ \ddot{y} \\ \ddot{z} \end{pmatrix} = \begin{pmatrix} \dot{y}p - \dot{z}w \sin \tau \\ -\dot{x}p + \dot{z}w \cos \tau \\ w \frac{d}{d\tau} (x \sin \tau - y \cos \tau) \end{pmatrix}. \tag{13}$$

The last equation can be integrated to give

$$\dot{z} = w(x \sin \tau - y \cos \tau) + c_z, \tag{14}$$

with integration constant c_z . The form of the equations above suggests trying a rotating coordinate system,

$$\begin{aligned} u &= x \cos \tau + y \sin \tau, \\ v &= y \cos \tau - x \sin \tau, \end{aligned} \tag{15}$$

$$\begin{aligned} \dot{u} &= \dot{x} \cos \tau + \dot{y} \sin \tau + v, \\ \dot{v} &= \dot{y} \cos \tau - \dot{x} \sin \tau - u, \end{aligned} \tag{16}$$

$$\begin{aligned} \ddot{u} &= \dot{x} \cos \tau + \dot{y} \sin \tau + 2\dot{v} + u, \\ \ddot{v} &= \dot{y} \cos \tau - \dot{x} \sin \tau - 2\dot{u} + v. \end{aligned} \tag{17}$$

After some algebra, this leads to a system of linear differential equations in the rotating coordinates u and v

$$\begin{aligned} \ddot{u} - (p+1)u &= (2+p)\dot{v}, \\ \ddot{v} - (p+1-w^2)v &= -(2+p)\dot{u} + wc_z, \\ \dot{z} &= -wv + c_z, \end{aligned} \tag{18}$$

which are the same set of equations of motion described in Fisch and Watanabe.¹⁴

B. General solution to the equations of motion

The linear system, Eq. (18), has two frequencies of oscillation,

$$a_{0,1}^2 = \frac{1}{2} (1 + (p+1)^2 + w^2) \pm \frac{1}{2} \sqrt{(p+2)^2(p^2 + 2w^2) + w^4}, \tag{19}$$

where a_0^2 corresponds to the $-$ sign, and a_1^2 to the $+$ sign. For stability, we require that $a_0^2 > 0$, which leads to the stability condition,

$$(1+p)(1+p-w^2) > 0, \tag{20}$$

which has to be satisfied for both electrons and ions. Now straying from the original paper,¹⁴ we now wish to look at all possible initial conditions for particles, without making any assumptions on what a typical orbit looks like. For notational convenience, we define

$$A_i \equiv \frac{a_i^2 + p + 1}{a_i(p+2)}. \tag{21}$$

To convert from our rotating coordinates $(u, \dot{u}, v, \dot{v}, \dot{z})$ back to Cartesian coordinates, we use matrix $T(\tau)$, which is the inverse of Eqs. (15) and (16),

$$T(\tau) = \begin{pmatrix} \cos \tau & 0 & -\sin \tau & 0 & 0 \\ -\sin \tau & \cos \tau & -\cos \tau & -\sin \tau & 0 \\ \sin \tau & 0 & \cos \tau & 0 & 0 \\ \cos \tau & \sin \tau & -\sin \tau & \cos \tau & 0 \\ 0 & 0 & 0 & 0 & 1 \end{pmatrix}. \tag{22}$$

For the general solution in rotating coordinates, we define matrix $V(\tau)$,

$$V(\tau) = \begin{pmatrix} s_0 & c_0 & s_1 & c_1 & 0 \\ a_0 c_0 & -a_0 s_0 & a_1 c_1 & -a_1 s_1 & 0 \\ A_0 c_0 & -A_0 s_0 & A_1 c_1 & -A_1 s_1 & \frac{w}{w^2 - p - 1} \\ -a_0 A_0 s_0 & -a_0 A_0 c_0 & -a_1 A_1 s_1 & -a_1 A_1 c_1 & 0 \\ -w A_0 c_0 & w A_0 s_0 & -w A_1 c_1 & w A_1 s_1 & \frac{-p-1}{w^2 - p - 1} \end{pmatrix}. \tag{23}$$

Before using information from initial conditions, we can show that orbits are uniquely defined by five time-independent parameters $\mu_A, \mu_B, \mu_C, \mu_D, c_z$,

$$\begin{pmatrix} x \\ \dot{x} \\ y \\ \dot{y} \\ \dot{z} \end{pmatrix} = T(\tau) \begin{pmatrix} u \\ \dot{u} \\ v \\ \dot{v} \\ \dot{z} \end{pmatrix} = T(\tau) V(\tau) \begin{pmatrix} \mu_A \\ \mu_B \\ \mu_C \\ \mu_D \\ c_z \end{pmatrix}. \tag{24}$$

These orbit parameters can be derived from the initial conditions at an arbitrary time τ_0 ,

$$\begin{pmatrix} \mu_A \\ \mu_B \\ \mu_C \\ \mu_D \\ c_z \end{pmatrix} = (T(\tau_0) V(\tau_0))^{-1} \begin{pmatrix} x \\ \dot{x} \\ y \\ \dot{y} \\ \dot{z} \end{pmatrix}_{\tau=\tau_0}, \tag{25}$$

where τ_0 can also be interpreted as the initial phase of the RMF. Putting the two equations together, we have the final solution of all possible orbits,

$$G(\tau, \tau_0) \equiv T(\tau) V(\tau) (T(\tau_0) V(\tau_0))^{-1}, \tag{26}$$

$$\begin{pmatrix} x \\ \dot{x} \\ y \\ \dot{y} \\ \dot{z} \end{pmatrix} = G(\tau, \tau_0) \begin{pmatrix} x \\ \dot{x} \\ y \\ \dot{y} \\ \dot{z} \end{pmatrix}_{\tau=\tau_0}. \tag{27}$$

C. Stability for both electrons and ions

We need to ensure that both electrons and ions simultaneously respect the stability condition in this electron orbit regime. Because

ions are much heavier than electrons, we can arrange for the situation where

$$\begin{aligned} p_e &< -1, \\ p_i + 1 &> w_i^2, \end{aligned} \quad (28)$$

where p_e denotes the value of p for electrons and p_i for ions. Note that only electron orbits can live in this $w^2 \gg 1$ regime while keeping both electron and ion orbits stable. Attempting to put ions in the same regime results in unstable electron orbits. We can now calculate the restriction this imposes on the magnitude of w_e . Using the ratio

$$R = -\frac{m_i/q_i}{m_e/q_e} = \mathcal{O}(10^3), \quad (29)$$

then $p_i = -p_e/R$ and $w_i = -w_e/R$, so

$$\begin{aligned} p_e &< -1, \\ |w_e| &< R\sqrt{1 - p_e/R}. \end{aligned} \quad (30)$$

This leaves plenty of room for a strong w_e .

III. SCATTERING

A. Motivation

Fisch and Watanabe¹⁴ calculated a single particle dissipation model with very specific initial conditions and assumed that all of the oscillating energy in an orbit is dissipated via scattering. We instead keep track of the net work done by the RMF on an electron orbit between two collision events for all possible orbits and consider a sequence of scatterings.

B. Electron-ion scattering

Building on the previously derived single particle motion, we will introduce an electron-ion scattering model. In this type of collision, in the ion frame of reference, electron kinetic energy is conserved, but momentum is not. The electron-ion collision rate is given by¹⁸

$$\begin{aligned} \nu_{ei} &= \frac{k}{v^3}, \\ k &= \frac{4\pi Z e^4 n_e \ln \Lambda}{(4\pi\epsilon_0)^2 m_e^2}, \end{aligned} \quad (31)$$

where n is the particle number density of the plasma, v is the speed of an electron in the ion frame of reference, and $\ln \Lambda$ is a correction due to long-range Coulomb interactions in the plasma, and can be taken as $\ln \Lambda \approx 10$ for a wide range of plasma conditions. Note that the electron's scattering cross section, and hence collision rate, decreases with v . In practice, an approximation we will make is that ν_{ei} is constant between collisions.

For our model, we will treat electron-ion collisions as instantaneous events which conserve electron kinetic energy and scatter them isotropically. This is similar to the prescription for some Monte Carlo simulations. We will then use this collision model to calculate the effects on the entire population of electron orbits.

IV. RESISTIVITY FROM ELECTRON-ION COLLISIONS

The majority of the kinetic energy of the single electron orbits is not necessarily contributing to the azimuthal current, and the direction of their motion varies greatly over a single pass around the central axis. In fact, we will show that the azimuthal current contribution

from a single electron is almost completely uncorrelated with its initial azimuthal velocity. Hence the effects of isotropic scattering from electron-ion collisions cannot be treated as resetting the azimuthal current contribution of electrons, because in the $w_e^2 \gg |p_e| \gg |w_e| \gg 1$ regime the majority possible orbits an electron could occupy will observe near synchronous drift with the RMF.

We will also show the existence of a subset for attractor orbits into which pitch-angle scattering will quickly drive electrons within the first few collision times. These attractor orbits will be integral in describing the dynamics of heating/cooling and expansion/contraction of the electron orbit population.

A. Work done on a population of electrons

Since we know the exact path an electron will take given its initial conditions, we can calculate the net work done by the RMF on the electron between times t_0 and $t_0 + \Delta t$ between two collision events, which can only be done by the RMF's associated axial electric field

$$\Delta W = -wm_e\omega^2 \int_{\tau_0}^{\tau_0+\Delta\tau} u(wv - c_z) d\tau, \quad (32)$$

where τ_0 can either be interpreted as the nondimensionalized initial conditions' starting time $\tau_0 = \omega t_0$, or as the initial phase of the RMF relative to the x -axis at time $t=0$. Substituting our expressions for u and v from Eq. (24), we recover

$$\begin{aligned} \Delta W = & -w^2 m_e \omega^2 \int_{\tau_0}^{\tau_0+\Delta\tau} d\tau \left[A_0 \mu_A \mu_B \cos 2a_0 \tau + A_1 \mu_C \mu_D \cos 2a_1 \tau \right. \\ & + \frac{1}{2} A_0 (\mu_A^2 - \mu_B^2) \sin 2a_0 \tau + \frac{1}{2} A_1 (\mu_C^2 - \mu_D^2) \sin 2a_1 \tau \\ & + A_1 \mu_A \mu_C s_0 c_1 - A_1 \mu_A \mu_D s_0 s_1 + A_1 \mu_B \mu_C c_0 c_1 - A_1 \mu_B \mu_D c_0 s_1 \\ & + A_0 \mu_C \mu_A s_1 c_0 - A_0 \mu_C \mu_B s_1 s_0 + A_0 \mu_D \mu_A c_1 c_0 - A_0 \mu_D \mu_B c_1 s_0 \\ & \left. + c_z \frac{(p+1)/w}{w^2 - p - 1} (\mu_A s_0 + \mu_B c_0 + \mu_C s_1 + \mu_D c_1) \right]. \end{aligned} \quad (33)$$

This expression is periodic in nature (since the two frequencies a_0 and a_1 are different), so the exact time at which the electron undergoes its next collision dictates whether the RMF will have performed overall positive/negative/zero work on it. Thus, we can conclude that in the absence of collisions, the RMF on average dissipates no net power on the electrons, which is to be expected from a closed-orbit solution. Hence, any overall heating must be due to collisions promoting electrons into higher-energy orbits.

We now seek to rigorously calculate the work done (and hence heating) on a population of electrons due to the presence of stochastic electron-ion collisions. To recover a useful expression for deriving resistivity of the plasma, we are interested in the expected work done by the RMF on a large randomized population of electrons. By assuming collisions are only electron-ion, and that they pitch-angle scatter electrons elastically and isotropically, we can recover the expected work done on electrons before a scattering event with this type of randomized velocity initial conditions along with uniformly random initial x, y coordinates. We will denote this averaging by $\langle \dots \rangle_{c,N}$ (i.e., averaging over velocities due to multiple collisions c and averaging over positions due to multiple particles N). Using Eq. (33), we can concisely write this average as follows:

$$\langle \Delta W \rangle_{c,N} = -w^2 m_e \omega^2 \int_{\tau_0}^{\tau_0 + \Delta\tau} d\tau \boldsymbol{\mu}^\dagger U(\tau) \boldsymbol{\mu}, \tag{34}$$

where $\boldsymbol{\mu}$ and $\boldsymbol{\mu}^\dagger$ are defined as

$$\boldsymbol{\mu} = \begin{bmatrix} \langle \mu_A \rangle_{c,N} \\ \langle \mu_B \rangle_{c,N} \\ \langle \mu_C \rangle_{c,N} \\ \langle \mu_D \rangle_{c,N} \\ \langle c_z \rangle_{c,N} \end{bmatrix}, \quad (\boldsymbol{\mu}^\dagger)^T = \begin{bmatrix} \langle \mu_A \rangle_{c,N} \\ \langle \mu_B \rangle_{c,N} \\ \langle \mu_C \rangle_{c,N} \\ \langle \mu_D \rangle_{c,N} \\ \langle c_z \rangle_{c,N} \end{bmatrix}, \tag{35}$$

and the symmetric matrix $U(\tau)$ is given by

$$\frac{1}{2} \begin{bmatrix} A_0 \sin 2a_0 \tau & A_0 \cos 2a_0 \tau & A_1 s_0 c_1 + A_0 c_0 s_1 & A_0 c_0 c_1 - A_1 s_0 s_1 & \frac{(p+1)/w}{w^2 - p - 1} s_0 \\ 2U_{12} & -A_0 \sin 2a_0 \tau & A_1 c_0 c_1 - A_0 s_0 s_1 & -A_0 s_0 c_1 - A_1 c_0 s_1 & \frac{(p+1)/w}{w^2 - p - 1} c_0 \\ 2U_{13} & 2U_{23} & A_1 \sin 2a_1 \tau & A_1 \cos 2a_1 \tau & \frac{(p+1)/w}{w^2 - p - 1} s_1 \\ 2U_{14} & 2U_{24} & 2U_{34} & -A_1 \sin 2a_1 \tau & \frac{(p+1)/w}{w^2 - p - 1} c_1 \\ 2U_{15} & 2U_{25} & 2U_{35} & 2U_{45} & 0 \end{bmatrix}. \tag{36}$$

We now use Eq. (25) and the fact that all odd quantities and their combinations of the initial condition velocities average out to zero (e.g., $\langle \dot{x} \dot{y} \rangle_{c,N} = 0$) to calculate the expected work done under collisions. These restrictions on the initial conditions can be written in the form of a diagonal matrix X in the non-rotating frame,

$$X \equiv \mathbf{x} \mathbf{x}^\dagger = \begin{bmatrix} \frac{1}{2} r_0^2 & 0 & 0 & 0 & 0 \\ 0 & \frac{1}{3} v_0^2 & 0 & 0 & 0 \\ 0 & 0 & \frac{1}{2} r_0^2 & 0 & 0 \\ 0 & 0 & 0 & \frac{1}{3} v_0^2 & 0 \\ 0 & 0 & 0 & 0 & \frac{1}{3} v_0^2 \end{bmatrix}, \tag{37}$$

where r_0 and v_0 indicate the radius and the ω -normalized speed of the electron immediately after the collision event, and \mathbf{x} and \mathbf{x}^\dagger are defined as

$$\mathbf{x}(\tau_0) = \begin{bmatrix} \langle x \rangle_{c,N} \\ \langle \dot{x} \rangle_{c,N} \\ \langle y \rangle_{c,N} \\ \langle \dot{y} \rangle_{c,N} \\ \langle z \rangle_{c,N} \end{bmatrix}_{\tau=\tau_0}, \quad (\mathbf{x}^\dagger(\tau_0))^T = \begin{bmatrix} \langle x \rangle_{c,N} \\ \langle \dot{x} \rangle_{c,N} \\ \langle y \rangle_{c,N} \\ \langle \dot{y} \rangle_{c,N} \\ \langle \dot{z} \rangle_{c,N} \end{bmatrix}_{\tau=\tau_0}. \tag{38}$$

Without loss of generality we can set τ_0 to zero. This is because τ_0 indicates the starting phase of orbits relative to the RMF immediately after a collision n , the effects of which we have already averaged out with our $\langle \dots \rangle_N$ particle averaging. Using these equations along with the inverse V matrix all evaluated at $\tau_0 = 0$, we can find the collision-particle averaged orbit parameters in terms of the collision-particle averaged initial conditions, along with taking advantage of the fact that $\boldsymbol{\mu}$ and $\boldsymbol{\mu}^\dagger$ are time-independent between collision times.

$$\begin{aligned} \langle \Delta W \rangle_{c,N} &= -w^2 m_e \omega^2 \boldsymbol{\mu}^\dagger \left(\int_0^{\Delta\tau} d\tau U(\tau) \right) \boldsymbol{\mu} \\ &= -w^2 m_e \omega^2 \mathbf{x}(0)^T (S^{-1})^T \left(\int_0^{\Delta\tau} d\tau U(\tau) \right) S^{-1} (\mathbf{x}(0)^\dagger)^T \\ &= -w^2 m_e \omega^2 \text{Tr} \left[\left(\int_0^{\Delta\tau} d\tau U(\tau) \right) S^{-1} X (S^{-1})^T \right], \end{aligned} \tag{39}$$

where $S = T(0)V(0)$. This equation describes a stochastic process where the collision-particle expected initial speed after collision $n + 1$ is determined by the randomized time between collisions $\Delta\tau_n$ and the initial radius and speed after collision n ,

$$\begin{aligned} \langle v_{0,n+1}^2 \rangle_{c,N} - \langle v_{0,n}^2 \rangle_{c,N} &= \text{Tr} \left[(U^*(\Delta\tau_n) - U^*(0)) S^{-1} X'(\tilde{\gamma}_n) (S^{-1})^T \right] \langle r_{0,n}^2 \rangle_{c,N}, \end{aligned} \tag{40}$$

where $\tilde{\gamma}_n \equiv \langle v_{0,n}^2 \rangle_{c,N} / \langle r_{0,n}^2 \rangle_{c,N}$, and $U^*(\tau)$, $X'(\gamma)$ are defined as

$$\begin{aligned} U^*(\tau_1) - U^*(\tau_0) &= -w^2 \int_{\tau_0}^{\tau_1} d\tau U(\tau), \\ X'(\gamma) &= X_1 + \frac{2}{3} \gamma X_2 = \begin{bmatrix} 1 & 0 & 0 & 0 & 0 \\ 0 & \frac{2}{3} \gamma & 0 & 0 & 0 \\ 0 & 0 & 1 & 0 & 0 \\ 0 & 0 & 0 & \frac{2}{3} \gamma & 0 \\ 0 & 0 & 0 & 0 & \frac{2}{3} \gamma \end{bmatrix}. \end{aligned} \tag{41}$$

The last thing we need to complete this calculation is writing the stochastic process for the radius squared $r_{0,n}^2$, which we can also recover from the general orbit solution and performing collision-particle averaging like we did for the work done by the RMF,

$$r^2(\tau) = (\mu_A s_0 + \mu_B c_0 + \mu_C s_1 + \mu_D c_1)^2 + \left(\mu_A A_0 c_0 - \mu_B A_0 s_0 + \mu_C A_1 c_1 - \mu_D A_1 s_1 + c_z \frac{w}{w^2 - p - 1} \right)^2$$

$$\Rightarrow \langle \Delta r^2 \rangle_{c,N} = \boldsymbol{\mu}^\dagger (K(\Delta\tau) - K(0)) \boldsymbol{\mu} \Rightarrow \langle r_{0,n+1}^2 \rangle_{c,N} = \left(\frac{1}{2} \text{Tr} \left[(K(\Delta\tau_n) - K(0)) S^{-1} X'(\tilde{\gamma}_n) (S^{-1})^T \right] + 1 \right) \langle r_{0,n}^2 \rangle_{c,N}, \quad (42)$$

where the symmetric matrix $K(\tau)$ is given by

$$\begin{bmatrix} s_0^2 + A_0^2 c_0^2 & \frac{1}{2}(1 - A_0^2) \sin 2a_0 \tau & s_0 s_1 + A_0 A_1 c_0 c_1 & s_0 c_1 - A_0 A_1 c_0 s_1 & \frac{w A_0 c_0}{w^2 - p - 1} \\ K_{12} & c_0^2 + A_0^2 s_0^2 & c_0 s_1 - A_0 A_1 s_0 c_1 & c_0 c_1 + A_0 A_1 s_0 s_1 & \frac{-w A_0 s_0}{w^2 - p - 1} \\ K_{13} & K_{23} & s_1^2 + A_1^2 c_1^2 & \frac{1}{2}(1 - A_1^2) \sin 2a_1 \tau & \frac{w A_1 c_1}{w^2 - p - 1} \\ K_{14} & K_{24} & K_{34} & c_1^2 + A_1^2 s_1^2 & \frac{-w A_1 s_1}{w^2 - p - 1} \\ K_{15} & K_{25} & K_{35} & K_{45} & \frac{w^2}{(w^2 - p - 1)^2} \end{bmatrix}. \quad (43)$$

Note that the diagonal elements of K survive under τ -averaging, unlike the U matrix. We can now write the full stochastic process over the entire electron population for r_0^2 and v_0^2 with Eqs. (40) and (42) in the continuous random variable $\Delta\tau_n$,

$$\langle v_{0,n+1}^2 \rangle_{c,N} = \left(\text{Tr} \left[(U^*(\Delta\tau_n) - U^*(0)) S^{-1} X'(\tilde{\gamma}_n) (S^{-1})^T \right] + \tilde{\gamma}_n \right) \langle r_{0,n}^2 \rangle_{c,N},$$

$$\langle r_{0,n+1}^2 \rangle_{c,N} = \left(\frac{1}{2} \text{Tr} \left[(K(\Delta\tau_n) - K(0)) S^{-1} X'(\tilde{\gamma}_n) (S^{-1})^T \right] + 1 \right) \langle r_{0,n}^2 \rangle_{c,N}. \quad (44)$$

Because many electrons will be colliding with ions at different randomized times, we can average this stochastic process over $\Delta\tau$ to get the overall expected changes in electron radius and speed. In essence, we seek to recover the following deterministic process,

$$\langle v_{0,n+1}^2 \rangle_{\Delta\tau,c,N} = \left(\text{Tr} \left[\langle U^*(\Delta\tau_n) - U^*(0) \rangle_{\Delta\tau} S^{-1} X'(\gamma_n) (S^{-1})^T \right] + \gamma_n \right) \langle r_{0,n}^2 \rangle_{\Delta\tau,c,N},$$

$$\langle r_{0,n+1}^2 \rangle_{\Delta\tau,c,N} = \left(\frac{1}{2} \text{Tr} \left[\langle K(\Delta\tau_n) - K(0) \rangle_{\Delta\tau} S^{-1} X'(\gamma_n) (S^{-1})^T \right] + 1 \right) \langle r_{0,n}^2 \rangle_{\Delta\tau,c,N}, \quad (45)$$

where $\gamma_n \equiv \langle v_{0,n}^2 \rangle_{\Delta\tau,c,N} / \langle r_{0,n}^2 \rangle_{\Delta\tau,c,N}$. To perform this averaging, we will need to know how $\Delta\tau_n$ is distributed. For a given electron temperature, the continuous random variable $\Delta\tau_n$ is exponentially distributed

$$P(\Delta\tau_n) = \lambda e^{-\lambda \Delta\tau_n},$$

$$\lambda = \nu_{ei} / \omega, \quad (46)$$

where ν_{ei} indicates the electron-ion collision rate. It is distributed this way because the probability of an electron undergoing a collision in the time interval $[\Delta\tau_n, \Delta\tau_n + d(\Delta\tau_n)]$ and no earlier is equal to the product of $e^{-\lambda \Delta\tau_n}$ (the probability that no collisions occur for $\Delta\tau_n$ amount of time) and $\lambda d(\Delta\tau_n)$ (the probability of a collision occurring in the subsequent interval $[\Delta\tau_n, \Delta\tau_n + d(\Delta\tau_n)]$). Note that we will be treating ν_{ei} as constant in time for this calculation, which is not true, in general, since it scales with v^{-3} . However, we will find that in the collisionless limit (i.e., allowing electrons to complete at least a few orbits on average before a collision event) that this approximation holds as shown in Figs. 1 and 2. The integrals involved in this averaging are notably in the form of Laplace transforms, so we can write the expressions as follows:

$$\langle v_{0,n+1}^2 \rangle_{\Delta\tau,c,N} = \left(\text{Tr} \left[\lambda \mathcal{L}_s [U^*(s) - U^*(0)] (\lambda) S^{-1} X'(\gamma_n) (S^{-1})^T \right] + \gamma_n \right) \langle r_{0,n}^2 \rangle_{\Delta\tau,c,N},$$

$$\langle r_{0,n+1}^2 \rangle_{\Delta\tau,c,N} = \left(\frac{1}{2} \text{Tr} \left[\lambda \mathcal{L}_s [K(s) - K(0)] (\lambda) S^{-1} X'(\gamma_n) (S^{-1})^T \right] + 1 \right) \langle r_{0,n}^2 \rangle_{\Delta\tau,c,N}. \quad (47)$$

In the low collisionality limit $\lambda = \nu_{ei} / \omega \ll a_0$, i.e., when orbits are allowed to perform at least a few cycles before a collision event, the random variable $\Delta\tau_n$ gets so large that the time of the previous collision no longer affects the process. Working in this limit yields

$$\lim_{\lambda \rightarrow 0} \lambda \mathcal{L}_s[U^*(s) - U^*(0)](\lambda) = -\frac{w^2}{2} \begin{bmatrix} \frac{A_0}{2a_0} & 0 & \frac{a_1 A_0 - a_0 A_1}{a_1^2 - a_0^2} & 0 & \frac{1}{a_0} \frac{(p+1)/w}{w^2 - p - 1} \\ 0 & -\frac{A_0}{2a_0} & 0 & \frac{a_0 A_0 - a_1 A_1}{a_1^2 - a_0^2} & 0 \\ \frac{a_1 A_0 - a_0 A_1}{a_1^2 - a_0^2} & 0 & \frac{A_1}{2a_1} & 0 & \frac{1}{a_1} \frac{(p+1)/w}{w^2 - p - 1} \\ 0 & \frac{a_0 A_0 - a_1 A_1}{a_1^2 - a_0^2} & 0 & -\frac{A_1}{2a_1} & 0 \\ \frac{1}{a_0} \frac{(p+1)/w}{w^2 - p - 1} & 0 & \frac{1}{a_1} \frac{(p+1)/w}{w^2 - p - 1} & 0 & 0 \end{bmatrix}, \tag{48}$$

$$\lim_{\lambda \rightarrow 0} \lambda \mathcal{L}_s[K(s) - K(0)](\lambda) = \begin{bmatrix} \frac{1}{2}(1 - A_0^2) & 0 & -A_0 A_1 & 0 & A_0 \frac{-w}{w^2 - p - 1} \\ 0 & -\frac{1}{2}(1 - A_0^2) & 0 & -1 & 0 \\ -A_0 A_1 & 0 & \frac{1}{2}(1 - A_1^2) & 0 & A_1 \frac{-w}{w^2 - p - 1} \\ 0 & -1 & 0 & -\frac{1}{2}(1 - A_1^2) & 0 \\ A_0 \frac{-w}{w^2 - p - 1} & 0 & A_1 \frac{-w}{w^2 - p - 1} & 0 & 0 \end{bmatrix}.$$

Combining Eqs. (47) and (48) gives us a full analytic expression for how the entire electron population heats/cool and expands/contracts under electron-ion pitch-angle scattering, which we can use to derive how the entire system heats/cool and expands/contracts under collisions.

B. γ_∞ -attractor orbits

The form of Eq. (47) implies the existence of a preferred speed-radius ratio,

$$\gamma_\infty \equiv \lim_{n \rightarrow \infty} \frac{\langle v_{0,n}^2 \rangle_{\Delta\tau,c,N}}{\langle r_{0,n}^2 \rangle_{\Delta\tau,c,N}}, \tag{49}$$

that the system of orbits is attracted to after each particle undergoes a few pitch-angle scatter events. Using Eqs. (47) and (48), we find that in the low collisionality limit this fixed point is determined explicitly by

$$\frac{2}{3} k_2 \gamma_\infty^2 + \left(k_1 - \frac{2}{3} u_2 \right) \gamma_\infty - u_1 = 0,$$

$$k_i \equiv \text{Tr} \left[\frac{1}{2} \lim_{\lambda \rightarrow 0} \lambda \mathcal{L}_s [K(s) - K(0)](\lambda) S^{-1} X_i (S^{-1})^T \right], \tag{50}$$

$$u_i \equiv \text{Tr} \left[\lim_{\lambda \rightarrow 0} \lambda \mathcal{L}_s [U^*(s) - U^*(0)](\lambda) S^{-1} X_i (S^{-1})^T \right],$$

where $X_1 + \frac{2}{3} \gamma X_2 = X'(\gamma)$. This gives us a quadratic equation for γ_∞ which in our case always gives a unique solution,

$$\gamma_\infty = \frac{-\left(k_1 - \frac{2}{3} u_2 \right) + \sqrt{\left(k_1 - \frac{2}{3} u_2 \right)^2 + \frac{8}{3} k_2 u_1}}{\frac{4}{3} k_2}. \tag{51}$$

The attractor orbits characterized by γ_∞ dictate the overall heating/cooling of the population of electrons. If the electron population starts at $\gamma > \gamma_\infty$, the electrons will undergo rapid cooling and expansion in the first few collision times in order to reach γ_∞ , and the opposite will occur when $\gamma < \gamma_\infty$. In a real experiment, we would expect the plasma to initially be cold, hence the plasma would start at $\gamma < \gamma_\infty$. This model predicts that the electrons would undergo rapid heating and contraction of orbits for the first ~ 10 collision times in order to reach γ_∞ . Once the equilibrium γ_∞ is reached, there remains only a slow heating rate given by

$$P_D = \frac{1}{2} g_\infty m_e \omega^2 n_e \nu_{ei} \langle v_{0,n}^2 \rangle_{\Delta\tau,c,N} = \frac{3}{2} g_\infty n_e T_e \nu_{ei} (T_e), \tag{52}$$

$$g_\infty \equiv \frac{\text{Tr} \left[\lim_{\lambda \rightarrow 0} \lambda \mathcal{L}_s [U^*(s) - U^*(0)](\lambda) S^{-1} X'(\gamma_\infty) (S^{-1})^T \right]}{\gamma_\infty}.$$

This power dissipation rate is derived by multiplying the increase in bulk electron kinetic energy density per collision $\frac{1}{2} g_\infty n_e m_e \omega^2 \langle v_{0,n}^2 \rangle_{\Delta\tau,c,N}$, calculated with recourse to Eq. (40), with the electron-ion collision rate ν_{ei} . We can refer to g_∞ as the γ -equilibrium heating/expansion rate as both $\langle r_{0,n}^2 \rangle_{\Delta\tau,c,N}$ and $\langle v_{0,n}^2 \rangle_{\Delta\tau,c,N}$ grow by a factor of $(1+g_\infty)$ per collision in the $\gamma = \gamma_\infty$ regime, i.e., they both grow slowly but geometrically,

$$\langle r_{0,m}^2 \rangle_{\Delta\tau,c,N} = \langle r_{0,n}^2 \rangle_{\Delta\tau,c,N} (1 + g_\infty)^{m-n}, \tag{53}$$

$$\langle v_{0,m}^2 \rangle_{\Delta\tau,c,N} = \langle v_{0,n}^2 \rangle_{\Delta\tau,c,N} (1 + g_\infty)^{m-n},$$

where collision count n is sufficiently large such that the system has already reached the $\gamma = \gamma_\infty$ equilibrium. In the limit of $|p_e| \gg 1$, $|w_e| \gg 1$, as shown in Fig. 3, γ_∞ and g_∞ reduce to

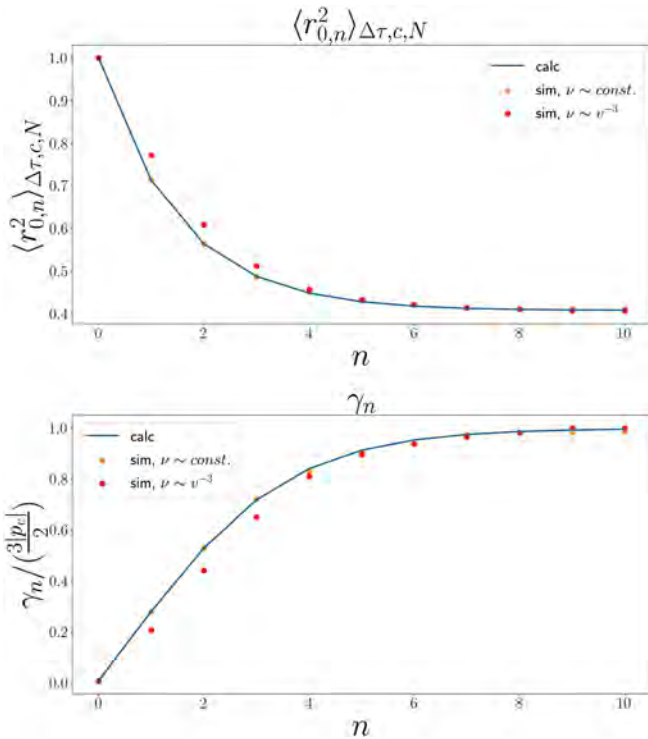


FIG. 1. Short-term evolution of electron orbit population radius $\langle r_{0,n}^2 \rangle_{\Delta\tau,c,N}$ and squared speed-radius ratio γ_n under collision n for electron machine parameters $\rho_e = -1.0 \times 10^3$, $w_e = -1.0 \times 10^2$, initializing with zero speed. The blue line represents the analytic result from Eqs. (47) and (48) while the orange and red points indicate the numerical results from direct simulation of 10 000 particles undergoing stochastic isotropic pitch-angle scattering with a constant and $\sim v^{-3}$ collision rate respectively, both with a mean collision rate of 0.1ω . This demonstrates that the approximation made in Eq. (46) is valid in this regime. Note that γ_n levels off to a predetermined constant $\gamma_\infty(\rho_e, w_e) \equiv \lim_{n \rightarrow \infty} \langle v_{0,n}^2 \rangle_{\Delta\tau,c,N} / \langle r_{0,n}^2 \rangle_{\Delta\tau,c,N}$ by rapidly heating electrons and contracting their orbits, which all occurs within ~ 10 collisions per electron. If electrons were instead initialized with a high energy such that $\gamma_0 > \gamma_\infty$, then the system would instead undergo rapid cooling and expansion in the first few collisions.

$$\begin{aligned} \gamma_\infty &= \frac{3|p_e|}{2}, \\ g_\infty &= \frac{4}{5|p_e|}, \end{aligned} \tag{54}$$

which yields a power density dissipation rate of

$$P_D = \frac{6}{5|p_e|} n_e T_e \nu_{ei}(T_e). \tag{55}$$

Note that the heating rate expression overall scales with $T_e^{-1/2}$ and intriguingly scales inversely with the background magnetic field strength B_0 , indicating a very slow heating rate that is independent from the RMF field strength B_\perp assuming it is sufficiently strong.

C. Azimuthal current and resistivity of a γ_∞ -population of electrons

The azimuthal current density J_θ is given by

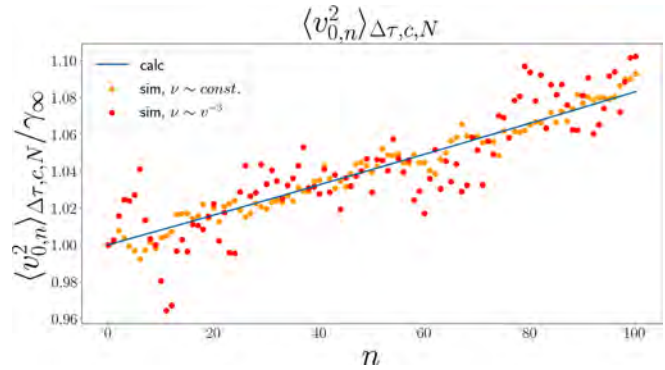


FIG. 2. Long-term gradual electron heating (and expansion) after the asymptotic γ_∞ is reached from both the analytic result in Eqs. (47) and (48) and direct numerical simulation with the same parameters used in Fig. 1 (except for using only 1000 particles rather than 10 000 for the v^{-3} collision rate). In this regime, the electron orbits undergo slow heating and expansion at a predetermined rate $g_\infty(\rho_e, w_e)$ as defined in Eq. (52).

$$J_\theta = -en_e \omega \langle \dot{\theta} r \rangle_{\Delta\tau,c,N}, \tag{56}$$

where $\dot{\theta}$ indicates the normalized azimuthal angular velocity such that $\dot{\theta} = 1$ would indicate perfect synchronous drift with the RMF. We currently do not have an analytic expression for $\langle \dot{\theta} r \rangle_{\Delta\tau,c,N}$, since it

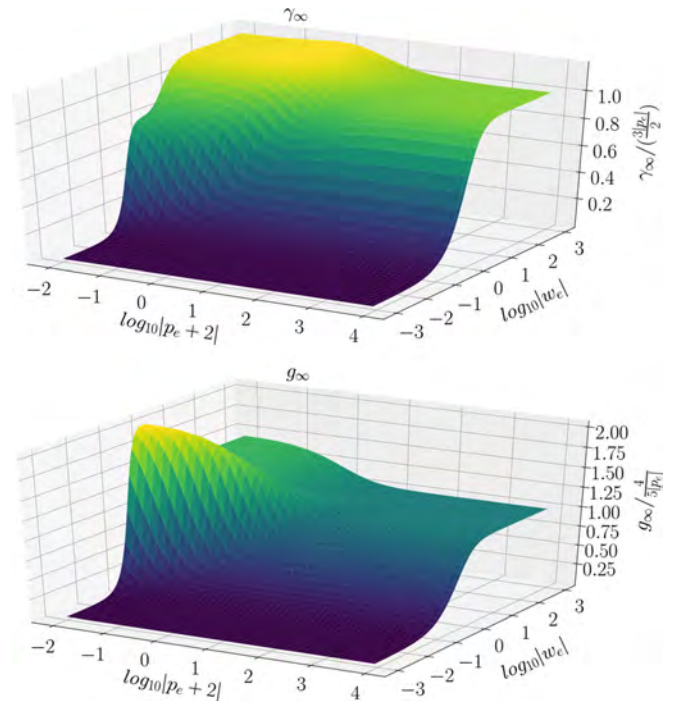


FIG. 3. Overall asymptotic speed-radius ratio $\gamma_\infty \equiv \lim_{n \rightarrow \infty} \langle v_{0,n}^2 \rangle_{\Delta\tau,c,N} / \langle r_{0,n}^2 \rangle_{\Delta\tau,c,N}$ and heating/expansion rate g_∞ of electron orbits undergoing electron-pitch-angle scattering plotted against varying electron machine parameters ρ_e , w_e . We find that as long as we are in the $\rho_e \gg 1$, $w_e \gg 1$ regime [while obeying the stability condition in Eq. (20)], the expressions found in Eq. (54) are valid.

involves a non-trivial time integral which is then averaged over isotropic initial conditions,

$$\langle \dot{\theta} r \rangle_{\Delta\tau, c, N} = \left\langle \lim_{T \rightarrow \infty} \frac{1}{T} \int_0^T d\tau \frac{x\dot{y} - y\dot{x}}{\sqrt{x^2 + y^2}} \right\rangle_{c, N}. \quad (57)$$

However, we can instead calculate this quantity numerically by initializing many particles with randomized isotropic positions and velocities whose initial conditions follow the γ_∞ speed-radius constraint in Eq. (51). In the $w_e^2 \gg |p_e| \gg |w_e| \gg 1$ regime, this quantity comes out to be approximately

$$\langle \dot{\theta} r \rangle_{\Delta\tau, c, N} \approx 0.7 \langle r \rangle_{\Delta\tau, c, N} \approx 0.7 \sqrt{\langle r^2 \rangle_{\Delta\tau, c, N}}, \quad (58)$$

which indicates a good overall synchronous drift with the RMF for all orbits in this regime.

We also find that the average azimuthal velocity cannot be approximated by the product of the average azimuthal angular velocity and radius,

$$\langle \dot{\theta} r \rangle_{\Delta\tau, c, N} \not\approx \langle \dot{\theta} \rangle_{\Delta\tau, c, N} \langle r \rangle_{\Delta\tau, c, N}. \quad (59)$$

Thus, it is misleading to characterize the current-generating capacity of an orbit based on its time-averaged azimuthal angular velocity alone. To get a better idea of the required machine size to contain these orbits, we also calculated the expected maximum radius of an orbit in relation to its time-averaged radius as

$$\langle r_{\max} \rangle_{\Delta\tau, c, N} \approx 1.3 \langle r \rangle_{\Delta\tau, c, N} \approx 1.2 \sqrt{\langle r^2 \rangle_{\Delta\tau, c, N}}. \quad (60)$$

With these numerical calculations, we can now solve for the azimuthal current density in terms of parameters we know analytically,

$$\begin{aligned} J_\theta &\approx -0.7 en_e \omega \sqrt{\langle r^2 \rangle_{\Delta\tau, c, N}} \\ &= -0.7 \sqrt{\frac{2}{3}} |p_e|^{-1/2} en_e \omega \sqrt{\langle v^2 \rangle_{\Delta\tau, c, N}} \\ &\approx -|p_e|^{-1/2} \frac{en_e}{m_e^{1/2}} T_e^{1/2}. \end{aligned} \quad (61)$$

We can then substitute this expression back into the previous equation and recover the power dissipation law,

$$P_D / J_\theta^2 \approx \frac{1.2}{|p_e|} \eta_{Sp}, \quad (62)$$

which is much smaller than both the Fisch–Watanabe¹⁴ and Hugarss–Klima resistivities.^{10–12} The non-dimensional prefactor in front of our equation is vanishingly small, which tells us that current drive ought to be very efficient in this $w_e^2 \gg |p_e| \gg |w_e| \gg 1$ electron regime, vastly outperforming the Spitzer resistivity.

V. DISCUSSION

The very large current drive efficiency, essentially a *mammoth* current drive efficiency, as summarized in Eq. (62), is certainly nonintuitive. In the regime in which it is large, it is even larger in the regime in which the perpendicular magnetic field is large, namely, where $|p_e| \gg 1$. In fact, the current in this limit appears to be essentially dissipationless, even while remaining finite. One might seek, therefore, to

compare this phenomenon with current drive efficiencies associated with other methods.

The original thinking advanced in the rotamak literature was that the current drive would be related to the momentum input by the wave^{10–12} much like advanced by Wort in the so-called *peristaltic* tokamak.¹⁹ In that picture, the azimuthal current is supported by azimuthal wave momentum. Thus, in this picture, since, for the same current, the energy input is proportional to the square of the velocity of the current carrier, while it is lost every collision time of the electrons, the law for energy dissipation becomes essentially the Spitzer or Ohmic resistivity. The same reasoning leads to other methodologies of pushing the bulk (thermal) electrons, but not the bulk ions, such as by low frequency waves²⁰ or neutral beams.²¹ However, in these other current drive mechanisms, including those featured in the peristaltic tokamak, as well as of course the Ohmic current drive mechanism, the current is driven in the direction of the magnetic field.

Here, the same reasoning is used to derive current drive efficiencies for current driven *perpendicular* to the main magnetic field. However, driving current perpendicular to a magnetic field is thought to be harder than driving current parallel to a magnetic field, whereas by Eq. (62), it appears to be easier to drive current perpendicular to a magnetic field. So the question arises, what might be the mechanisms to make current flow with less dissipation?

First, note that the classical resistivity perpendicular to a magnetic field is a factor of two more than the resistivity parallel to the magnetic field. This increases the dissipation compared to the Ohmic dissipation in driving currents parallel to the field, rather than explaining why the dissipation should be less. Although the picture of calculating the dissipation as though an electron fluid was simply dragged azimuthally was challenged by the initial single particle approach,¹⁴ which suggested that the large motions perpendicular to the azimuthal dragging of the electrons needed to be considered, taking those motions into account suggested more dissipation, rather than less dissipation, as found here.

Second, note that, in seeking much less dissipation, in the case of current drive efficiency parallel to a magnetic field, the smallest dissipation occurs when waves are arranged to resonate only with the superthermal electrons, such as by lower hybrid waves²² or electron cyclotron waves.²³ In both cases, it is not necessary that wave momentum drives the current; rather it is essential that the electrons carrying the current be substantially superthermal, so that they collide less. In principle, the efficiency can be made even larger by arranging the wave-particle resonance conditions such that electrons are pushed in a direction close to their constant energy surfaces.²⁴ However, as higher efficiency is sought in this manner, fewer electrons can be found that meet the necessary conditions, so, in practice, there is a limited amount of current that can be driven at very high efficiency. In any event, these methodologies pertain only to driving current parallel to a magnetic field.

Thus, to summarize, in the case of driving current parallel to the magnetic field, the picture is that particles receive an instantaneous push, and that results in current that lasts until a collision destroys that current. The efficiency can then be optimized by arranging for that current to last longer or for the energy required in the push to be less. The current lasts longer if the electrons carrying the current are faster. In all cases, the push is to higher energy, but the push requires less energy either if the electrons being pushed have less velocity in the direction of the push, or if the push is along constant energy surfaces.

In contrast, in driving current perpendicular to a magnetic field, such as in a rotamak, the current only exists while the wave excitation persists. There might be a push, but the current lasts only during the push itself; no current persists until destroyed by a collision as in the case of driving current parallel to the magnetic field. This situation is more analogous to the case of alpha channeling, where charge is pushed by waves across the magnetic field.²⁵ In the case of alpha channeling, which generally involves pushing ions across the field rather than electrons, there is the opportunity to extract energy from the particles (thereby amplifying the wave) even as the current is driven. The utilization of the particle's own kinetic energy suggests the appearance of a high efficiency in driving this current. However, the kinetic energy is released only because the particle is diffused by the wave in space to a position of lower phase space density, in the energy-configuration space. The alpha channeling effect also occurs in a rotating plasma, where some potential energy can also be released to drive the perpendicular current.²⁶ However, in the case of alpha channeling, whether in a rotating plasma or a non-rotating plasma, it is imprecise to define a steady state current drive efficiency, since the plasma itself is expanding rather than in steady state.

The fact that the rotamak orbits uncovered here both suggest very high current drive efficiency, but require a concomitant expansion of the plasma, suggests that the high efficiency case here might be analogous to the apparent high efficiencies in driving currents across magnetic fields through the alpha channeling effect, which also require plasma expansion while appearing to be highly efficient. However, the rotamak drive is different in that it is not a resonant effect targeting only a select group of particles. Also, in the presence of the rotating magnetic field, the magnetic field direction itself changes, so current that is perpendicular to the axial magnetic field is not exactly perpendicular to the instantaneous magnetic field. Moreover, it still remains mysterious why the efficiency is so high when the axial magnetic field is made stronger.

There are caveats to this high efficiency. First, the very high efficiency comes with the caveat that, as in the case of alpha channeling, it is not quite a steady state efficiency. It requires the plasma to expand, even if not so much. Second, the rotating field is assumed to penetrate the plasma fully, even in the very high efficiency regime where the axial field is made very large. The details of that penetration could affect the apparent current drive efficiency. For example, analogous to the case of currents driven by alpha channeling, bringing power from outside the plasma to drive the current (the boundary value problem), as opposed to damping waves interior to the plasma (the initial value problem), can result in very different currents in the plasma.²⁷ This difference occurs because the nonresonant particles that support the wave also can carry current. In some cases, this current can be substantial. A third caveat is that the collisions here are implemented as though each electron has a fixed energy between collision events. In fact, over an orbit, the electron energy varies. To the extent that electrons change their energy substantially in the wavefield, this approximation may need revisiting. Finally, it should be observed that if substantial current is generated, to the extent that the applied axial field is substantially canceled, then the conditions for efficient current generation would be violated.

On top of this, we also assumed a uniform axial field B_0 , which made electron orbits integrable. When a more realistic field is used,

electron orbits can become chaotic as they reach the boundaries of the confining field, even without the presence of an RMF.²⁸ That leads to very different non-integrable motion than what we have found here. Thus, it is not clear whether any effects found in this paper, such as the surprising low dissipation effect, would survive in full FRC field geometries. However, we do surmise that our low dissipation result would apply to electron orbits that stay away from any boundaries which would induce stochasticity even in the absence of collisions. Hence there may be a class of electron orbits which survive for long enough near the $z=0$ midplane which drive a sufficient azimuthal current and magnetic field in the $-z$ direction. In any event, whether or not the model here pertains to practical laboratory experimental geometries, the low dissipation effect uncovered within the idealized geometry remains surprising.

Despite these caveats, we are left in Eq. (62) with a mysterious, enormously high current drive efficiency, even if it requires assuming a penetrating driving field, even if a small amount of plasma expansion makes the driven current not quite steady state, and even if stochasticity inducing boundary conditions that occur in realistic geometries are neglected in the straight confining magnetic field geometry that we consider here.

VI. CONCLUSION

Using a single-particle motion picture with repeated stochastic electron-ion pitch-angle scattering, we have found very specific requirements for machine parameters on the electron orbits $w_e^2 \gg |p_e| \gg |w_e| \gg 1$, where the power dissipation required to maintain an azimuthal current becomes vanishingly small $\sim \eta_{sp}/|p_e|$ despite the presence of electron-ion collisions. This power dissipation can be significantly less than what either Fisch and Watanabe¹⁴ or Hugrass and Klima⁹⁻¹² would predict.

We have also found that collisions drive the system of electrons to a unique preferred speed-radius state γ_∞ initial deviation from which (under the previously specified machine parameters) will cause rapid expansion-cooling or contraction-heating to reach $\gamma_\infty = 3|p_e|/2$ within roughly 10 collision times, after which only very gradual $\propto 4/(5|p_e|)$ heating and expansion takes place.

ACKNOWLEDGMENTS

This work was supported by U.S. DOE Grant Nos. DE-AC02-09CH11466 and DE-SC0016072.

AUTHOR DECLARATIONS

Conflict of Interest

The authors have no conflicts to disclose.

DATA AVAILABILITY

Data sharing is not applicable to this article as no new data were created or analyzed in this study.

REFERENCES

- H. A. Blevin and P. C. Thonemann, "Plasma confinement using an alternating magnetic field," *Nucl. Fusion* **part 1**, 55 (1962).
- I. R. Jones, "A review of rotating magnetic field current drive and the operation of the rotamak as a field-reversed configuration (Rotamak-FRC) and a spherical tokamak (Rotamak-ST)," *Phys. Plasmas* **6**, 1950 (1999).

- ³W. N. Hugrass, I. R. Jones, K. F. McKenna, M. G. R. Phillips, R. G. Storer, and H. Tucek, "Compact torus configuration generated by a rotating magnetic field—The Rotamak," *Phys. Rev. Lett.* **44**, 1676 (1980).
- ⁴J. T. Slough and K. E. Miller, "Enhanced confinement and stability of a field-reversed configuration with rotating magnetic field current drive," *Phys. Rev. Lett.* **85**, 1444 (2000).
- ⁵T. Furukawa, K. Shimura, D. Kuwahara, and S. Shinohara, "Verification of azimuthal current generation employing a rotating magnetic field plasma acceleration method in an open magnetic field configuration," *Phys. Plasmas* **26**, 033505 (2019).
- ⁶H. Y. Guo, A. L. Hoffman, R. D. Milroy, L. C. Steinhauer, R. D. Brooks, C. L. Deards, J. A. Grossnickle, P. Melnik, K. E. Miller, and G. C. Vlases, "Improved confinement and current drive of high temperature field reversed configurations in the new translation, confinement, and sustainment upgrade device," *Phys. Plasmas* **15**, 056101 (2008).
- ⁷S. A. Cohen, B. Berlinger, C. Brunkhorst, A. Brooks, N. Ferraro, D. P. Lundberg, A. Roach, and A. H. Glasser, "Formation of collisionless high-beta plasmas by odd-parity rotating magnetic fields," *Phys. Rev. Lett.* **98**, 145002 (2007).
- ⁸H. K. Moffatt, "On fluid flow induced by a rotating magnetic field," *J. Fluid Mech.* **22**, 521 (1965).
- ⁹W. N. Hugrass, "Comments on the paper by N. J. Fisch, T. Watanabe 'Field reversal by rotating waves (Nucl. Fusion **22** (1982) 423)," *Nucl. Fusion* **22**, 1237 (1982).
- ¹⁰W. N. Hugrass, "Power and momentum relations in rotating magnetic-field current drive," *Aust. J. Phys.* **37**, 509 (1984).
- ¹¹R. Klima, "Nonlinear dragging of particles during high-frequency heating," *Plasma Phys. Controlled Fusion* **15**, 1031 (1973).
- ¹²R. Klima, "Angular-momentum transferred during electromagnetic energy-absorption and emission," *Czech. J. Phys. B* **24**, 846 (1974).
- ¹³W. A. Newcomb, "Motion of magnetic lines of force," *Ann. Phys.* **3**, 347–385 (1958).
- ¹⁴N. J. Fisch and T. Watanabe, "Field reversal by rotating waves," *Nucl. Fusion* **22**, 423 (1982).
- ¹⁵A. P. Kazantsev, "The motion of a charged particle in a rotating magnetic field," *Sov. Phys. JETP* **10**, 1036 (1960).
- ¹⁶A. Legatowicz, "Behaviour of plasma in a rotating magnetic field," *Nucl. Fusion* **1**, 155 (1961).
- ¹⁷T. Hatori and H. Washimi, "Covariant form of the ponderomotive potentials in a magnetized plasma," *Phys. Rev. Lett.* **46**, 240 (1981).
- ¹⁸F. F. Chen, *Introduction to Plasma Physics* (Springer, 1974).
- ¹⁹D. J. H. Wort, "Peristaltic Tokamak," *Plasma Phys.* **13**, 258 (1971).
- ²⁰N. J. Fisch and C. F. F. Karney, "Current generation with low-frequency waves," *Phys. Fluids* **24**, 27 (1981).
- ²¹T. Ohkawa, "New methods of driving plasma current in fusion devices," *Nucl. Fusion* **10**, 185 (1970).
- ²²N. J. Fisch, "Confining a tokamak plasma with Rf-driven currents," *Phys. Rev. Lett.* **41**, 873 (1978).
- ²³N. J. Fisch and A. H. Boozer, "Creating an anisotropic plasma resistivity with waves," *Phys. Rev. Lett.* **45**, 720 (1980).
- ²⁴N. J. Fisch, "Theory of current drive in plasmas," *Rev. Mod. Phys.* **59**, 175–234 (1987).
- ²⁵N. J. Fisch and J.-M. Rax, "Interaction of energetic alpha particles with intense lower hybrid waves," *Phys. Rev. Lett.* **69**, 612 (1992).
- ²⁶A. J. Fetterman and N. J. Fisch, " α channeling in a rotating plasma," *Phys. Rev. Lett.* **101**, 205003 (2008).
- ²⁷I. E. Ochs and N. J. Fisch, "Nonresonant diffusion in alpha channeling," *Phys. Rev. Lett.* **127**, 025003 (2021).
- ²⁸A. H. Glasser and S. A. Cohen, "Ion and electron acceleration in the field-reversed configuration with an odd-parity rotating magnetic field," *Phys. Plasmas* **9**, 2093 (2002).
- ²⁹S. A. Cohen, "Construction of the PFRC-2 device," in American Physical Society, 53rd Annual Meeting of the APS Division of Plasma Physics (2011).
- ³⁰S. A. Cohen and R. D. Milroy, "Maintaining the closed magnetic-field-line topology of a field-reversed configuration with the addition of static transverse magnetic fields," *Phys. Plasmas* **7**, 2539–2545 (2000).